sustainability

MDPI

Article

Assessment of CI Engine Performance and Exhaust Air Quality Outfitted with Real-Time Emulsion Fuel Injection System

Krishnamoorthy Ramalingam [1,*], Elumalai Perumal Venkatesan [2,3], Abdul Aabid [4] and Muneer Baig [4]

[1] Department of Mechanical Engineering, CK College of Engineering and Technology, Cuddalore 607003, India
[2] Department of Mechanical Engineering, Aditya Engineering College, Surampalem 533437, India; elumalaimech89@gmail.com
[3] Department of Mechanical Engineering, Jawaharlal Nehru Technological University Kakinada, East Godavari District, Kakinada 533003, India
[4] Department of Engineering Management, College of Engineering, Prince Sultan University, P.O. Box 66833, Riyadh 11586, Saudi Arabia; aaabid@psu.edu.sa (A.A.); mbaig@psu.edu.sa (M.B.)
* Correspondence: kskrishnamech@gmail.com; Tel.: +91-9698922334

Abstract: The main target of the current research work is effectively eliminating fossil fuel dependency and improving the exhaust air quality of conventional Compression Ignition (CI) engines. This research paper demonstrates for the first time that a nanofluid (water without surfactant) stored in separate tanks can be quantified, collected, and immediately emulsified by a high shear mixer before transfer into the combustion chamber of a diesel engine. The experiment was carried out under different load states (25%, 50%, 75% and 100%) with a constant speed of 1500 rpm. Biofuel was extracted from citronella leaves using an energy-intensive process. The 5% water share was used for preparing the biofuel emulsion and nano-biofuel emulsion. A cobalt chromate nanoadditive was used to make the nanofluid. An experimental investigation was performed with prepared test fuels, namely, ultra-low sulphur diesel (ULSD), 100% Citronella (B100), surfactant-free Diesel emulsion (SDE), surfactant-free bioemulsion (SBE), and Surfactant free nano-bioemulsion (SNBE), in a test engine. The properties of the sample test fuels was ensured according to EN and ASTM standards. The observation performance results show that the SNBE blend exhibited lower BTE (by 0.5%) and higher SFC (by 3.4%) than ULSD at peak load. The emission results show that the SNBE blend exhibited lower HC, CO, NO_x, and smoke emissions by 23.86%, 31.81%, 2.94%, and 24.63%, respectively, compared to USD at peak load. The CP and HRR results for SNBE were closer to ULSD fuel. Overall, the novel concept of an RTEFI (Real-time emulsion fuel injection) system was proved to be workable and to maintain its benefits of better fuel economy and greener emissions.

Keywords: nanofuel; diesel engine; emission; real-time emulsion fuel

check for updates

Citation: Ramalingam, K.; Perumal Venkatesan, E.; Aabid, A.; Baig, M. Assessment of CI Engine Performance and Exhaust Air Quality Outfitted with Real-Time Emulsion Fuel Injection System. *Sustainability* **2022**, *14*, 5313. https://doi.org/10.3390/su14095313

Academic Editor: Jorge Aburto

Received: 10 February 2022
Accepted: 8 April 2022
Published: 28 April 2022

Publisher's Note: MDPI stays neutral with regard to jurisdictional claims in published maps and institutional affiliations.

Copyright: © 2022 by the authors. Licensee MDPI, Basel, Switzerland. This article is an open access article distributed under the terms and conditions of the Creative Commons Attribution (CC BY) license (https://creativecommons.org/licenses/by/4.0/).

1. Introduction

Over the past twenty years, the rate of air pollution has grown rapidly and fossil fuels are becoming depleted due to the growth of industrialization and the drastic increase in the number of transport vehicles. The drain on global fossil energy sources is assessed as being likely to increase over the next ten years, and thought should be given to long-term utilization as well [1,2]. Among the many types of conversion equipment, the basic fuel engine has particular benefits, such as durability, reliability, power output, energy consumption, etc., Nevertheless, diesel fuel engines create high amounts of smoke emissions and nitrogen oxide [3,4]. At present, government emission regulations are very stringent in order to preserve human and environmental health. For these reasons, the scientific community seeks to discover renewable and emission-free alternate fuels for basic engines [5].

To satisfy energy demand, vegetable oil-based alternative fuels have received a great deal of consideration, as it is sustainable and non-toxic. Out of high viscous biofuel, today many researchers are attracted to the topic of low-viscosity biofuel because of its

thermo-chemical properties [6,7]. Among low-viscosity fuels, citronella fuel has received the attention of several researchers due to its abundant availability and high yield [8,9]. This vegetable-based biodiesel can be utilized in conventional engines with only minor alterations. In addition, biodiesel has enhanced physical–chemical properties compared to diesel, namely, its Cetane number, oxygen content, and absence of aroma [10,11].

The high oxygen content present in biodiesel prompts total ignition, which may cause lower HC as well as CO formation. On other hand, NO_x formation is increased due to elevated peak cylinder temperature, a negative obstacle for biodiesel use in diesel engines [12,13]. Nowadays, water in diesel or water in biodiesel as alternate energy is capable of significantly abating NO_x and smoke emissions [14]. The water in emulsified fuel minimizes the peak combustion flame temperature because of the high LHV of water, which results in diminished NO_x formation, and the positive effect of secondary atomization promotes better HC, CO, and smoke emission reduction in water–emulsion fuels. In addition, emulsion fuels show enhanced engine performance output response due to their improved air–fuel mixing rate, an effect of micro-explosion and atomization. Thus far, numerous kinds of water added to fuel have been introduced to base engines and their performance and emission output responses have been examined [15,16]. It has been shown that 20% water in diesel fuel emits lower PM and nitrogen oxide emissions by 40% and 50%, respectively, compared to base fuel [17]. In [18], the durability of a base engine fuelled with two different water proportions of emulsion fuel, namely E10 and E20, was evaluated. The test engine was operated for 200hrs energized with both water emulsion fuel, and the results showed a lower carbon store with 60% and half decrease for E10 and E20 fuel correspondingly compared to other emulsions.

Nevertheless, water in oil mixture fuels have one major downside, phase separation, which presents obstacles in the attempt to commercialize this technology. In order to stabilize the water in oil mixture, a surfactant is typically used [19]. Over the past decade, numerous researchers have conducted work to identify the optimal surfactant for a stable water–emulsion fuel. Several researchers have already managed to form stable water in oil emulsion fuels. However, it is costly, and moreover it requires an enormous volume of chemicals and additives, and the process is very tedious [20,21]. Water in oil emulsion fuels can probably be readied and supplied into the engine without of surfactant by persistently blending oil with water employing an in-line blending chamber in front of the delivered emulsion fuel provided to the engine chamber [22]. Ithnin first initiated the investigation into non-surfactant water emulsions with a base fuel in a base engine. The results show better improvement in efficiency and tailpipe emissions compared to diesel fuel, especially for NO_x and smoke [23]. The water emulsion fuel had higher HC and CO concentrations when increasing the particular limit of water concentration, because higher ignition lag correlates with water emulsion fuel [24]. In this respect, various adaptations have been made to diminish the ignition delay, such as nanoadditives, metal-based additives, etc., among which nanoadditives have shown the better results [25]. Most commonly, nanoadditives have specific functions to perform, namely, diminishing engine tailpipe emissions, enhancing fuel stability over a long period, lessening flash point and ignition delay, and increasing oxygent content. In addition, nanoadditives have a low melting point, high surface area, better heat and mass transfer, good thermal conductivity, and good oxidation [26–28], and are used as performance-enhancing catalysts in diesel engines [29].

Of the numerous possible nanoadditives, cobalt chromate was chosen for the current research work owing to its low cost, good thermal properties, and non-hazardous nature. This research paper aims to evaluate the effect of emulsifier-free nanoemulsion fuels in a diesel engine. A real-time emulsion fuel injection system (RTEFI) was created and connected near the fuel supply arrangement of the engine. In the current work, a mono-cylinder four-stroke CI engine was used under five different load states (25%, 50%, 75%, and 100%) at a constant speed of 1500 rpm. As a comparison, surfactant-free nanoemulsion (SNE), surfactant-free diesel emulsion (SDE), and diesel (D) fuels were tested. The 5% water share was used for both the nanofluid and diesel. The cobalt chromate nanoadditive was used

for making the nanofluid. In the test rig analysis, the BTE, CP, HRR and fuel utilization are discussed elaborately. The emission output responses, namely HC, CO, NO_x and, smoke, are discussed in detail. A comparison of the performance and emission responses of the assorted nanofuel combinations and diesel is shown in Table 1

Table 1. Comparison of performance and emission responses for assorted nanofuel combinations and diesel.

Type of Fuel Blend	Performance		Emission Characteristics				Ref.
	BSFC	BTE	CO	NO_x	HC	PM/Smoke	
Jatropha (Al_2O_3) 100 ppm	↓	↑	↓	↓	↓	↓	[30]
Jatropha (Ti) 100 ppm	↓	↑	↓	↓	↓	↓	[30]
Jatropha (CNT) 100 ppm	↓	↑	↓	↓	↓	↓	[30]
Oenothera (GO) 100 ppm	↓	↑	↓	↑	↓	↓	[31]
Garcinia gummi (CeO_2, ZrO_2, TiO_2)	↓	↑	↓	↑	↓	↓	[32]
WCO (CeO_2 80 ppm)	↓	↑	↓	↑	↓	↓	[33]
Neat Palm Oil (SiO_2) 10 and 20 ppm	↓	↑	↓	↑	↓	↓	[34]
Biodiesel—diesel (CNT, Ago 10, 20, 30 ppm)	↓	↑	↓	↑	↓	↓	[35]
WCO—Diesel (CNT 20, 40 and 100 ppm)	↓	↑	↓	↑	↓	↓	[36]
WOP (TiO_2) 100 ppm	↓	↑	↓	↓	↓	↓	[37]
Soyabean nanoemulsion (ZrO_2) 100 ppm	↓	↑	↓	↓	↓	↓	[38]
Nanoemulsion with Biodiesel (CNT 150 ppm)	↓	↑	↓	↑	↓	↓	[39]
Mustard oil—nanoemulsion (TiO_2) 50 ppm	↓	↑	↓	↓	↓	↓	[40]
Rice bran—nanoemulsion ($FeCl_2$)	↓	↑	↓	↓	↓	↓	[41]
Crude oil—nanoemulsion (Al_2O_3) 80 ppm	↓	↑	↓	↓	↓	↓	[42]

2. Materials and Method

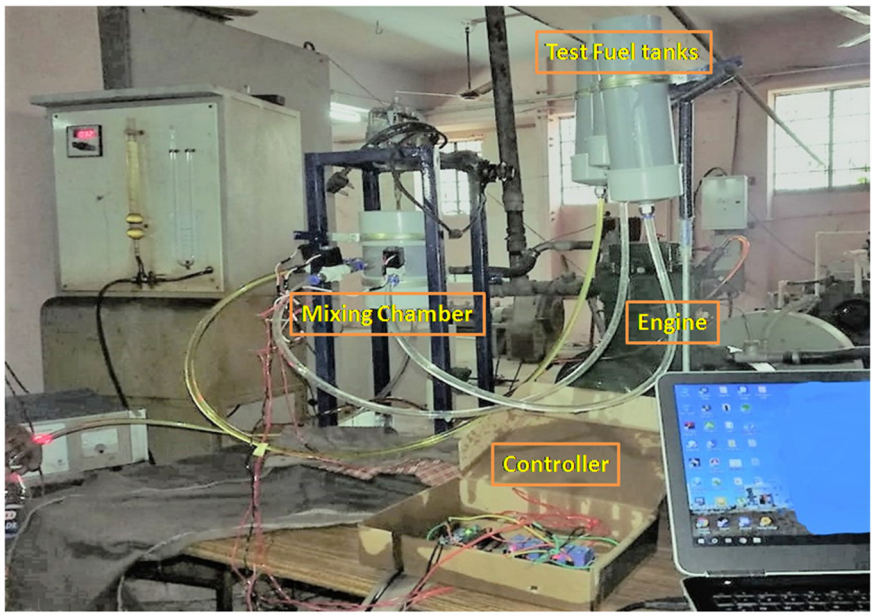
2.1. Configuration of RTEFI

Figure 1 exposes the arrangement of the real-time mixing system or RTEFI. Emulsifier-free emulsion fuel is prepared and supplied from this system to the engine, where fuel from the fuel tank is fed into a real-time mixing chamber through the fuel line. The filtered water or nanopowder-mixed water is injected into a real-time mixing system via a water injector from the tank. Initially, the immiscible liquids (water and oil) are homogenously mixed in a greater mixing chamber which responds to a high-power stator and rotator. The prepared emulsion fuel is then supplied to an ultrasonic transducer for introducing vigorous ultrasonic waves before the emulsifier-free emulsion fuel flows through into the diesel engine via the emulsion fuel supply line. The more prominent shear blenders and ultrasonic transducers are set by the regulator. The solenoid valve is used to control the supply of the water and oil fraction, which is shown in Figure 1 as well. The RTEFI system was placed closer to the fuel feed arrangement of the engine in order to eliminate separation of the prepared fuel phase.

2.2. Preparation and Characterization of Citronella Oil

Citronella (*Cymbopogon nardus*) oil was extracted through an energy-intensive process. The layout out of the energy-intensive setup is shown in Figure 2. Figures 3 and 4 inform the chemical bonds, structure, and functional group present in Cymbopogon nardus oil. A complete study was previously made in our earlier publication (Krishnamoorthy et al. [30]) of oil extraction, FTIR, and GCMS.

(**a**)



(**b**)

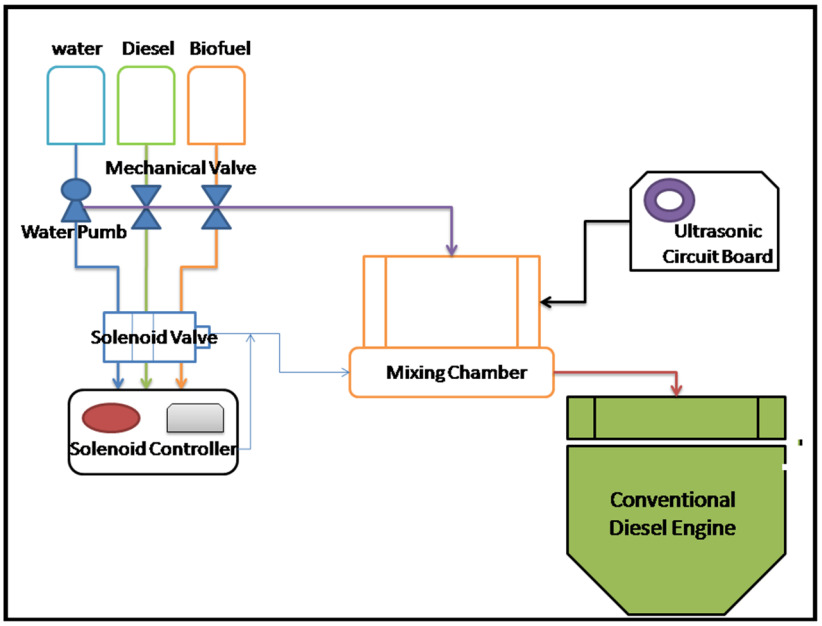


Figure 1. Configuration of RTEFIS: (**a**) pictographic representation of RTEFIS setup and (**b**) schematic representation.

2.3. Synthesis of Cobalt Chromite ($COCr_2O_4$) Nanoadditive

A redox solution at 250 °C, the commencement of solution combustion, and the end product are the three steps in this process. In a 1000 mL borosilicate container, cobalt (II) nitrate hexahydrate ($Co(NO_3)_2 \cdot 6H_2O$, Sigma-Aldrich 99% Purity) and chromium (III) nitrate nonahydrate ($Cr(NO_3)_3 \cdot 9H_2O$, Sigma-Aldrich 99% purity) were taken as the respective starting materials according to stoichiometric requirements, and were dissolved in the minimum amount of deionized water with continuous stirring. Then, a reducing agent of glycine fuel was added to the aforementioned solution and the solution was stirred at 200 rpm for 15 to 30 min. After that, the solution was heated with a hotplate and the temperature was elevated to 90 °C to allow for the gradual evaporation of water until a gel was produced. Furthermore, the gel was steadily heated to 200 °C until a flame and gas

combustion reaction was accomplished in less than 60 s. The resulting powders were calcinated in air at 500 °C for 5 h and subsequently furnace cooled. After cooling, the resulting materials ($CoCr_2O_4$, as Co^{2+} and Cr^{3+} ions occupied the A and B sites, respectively) were subjected to grinding via ball milling.

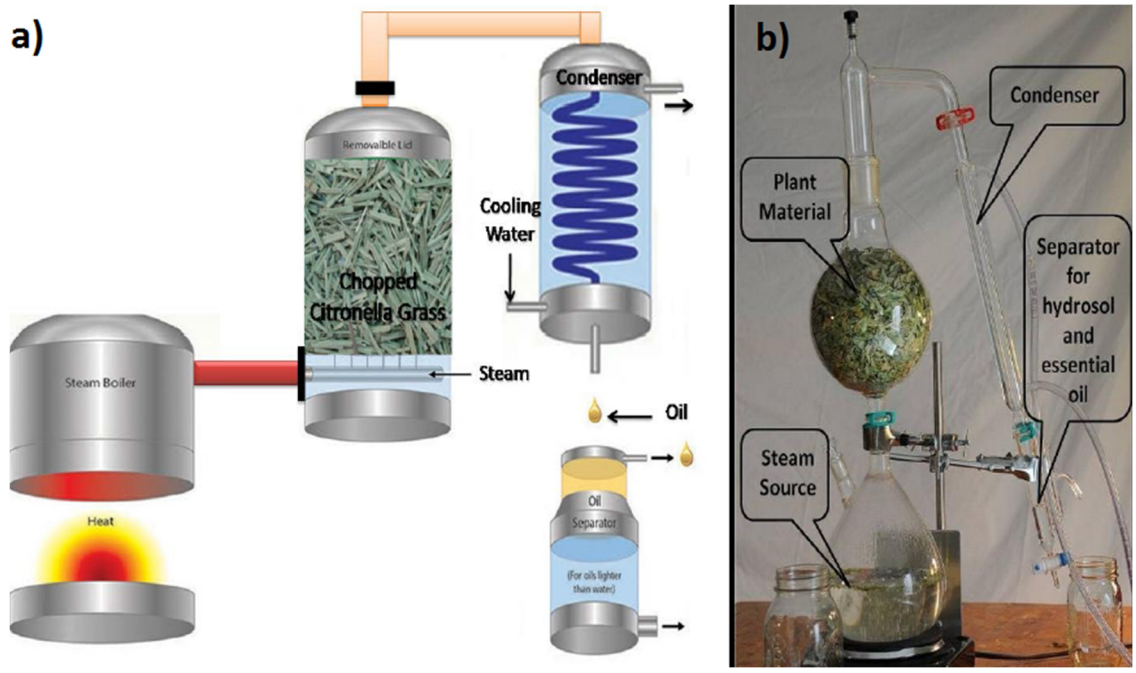


Figure 2. (**a**) Schematic of energy-intensive process and (**b**) photograph of energy-intensive process.

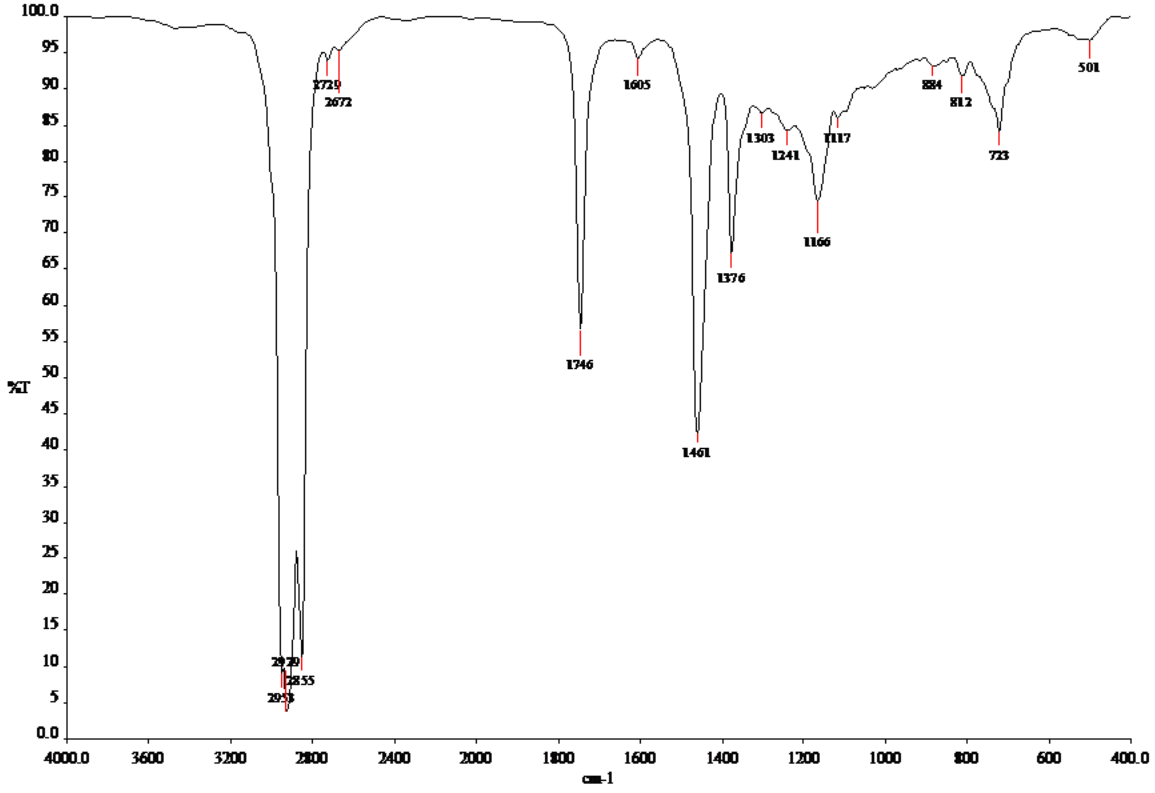


Figure 3. FT-IR for Citronella oil.

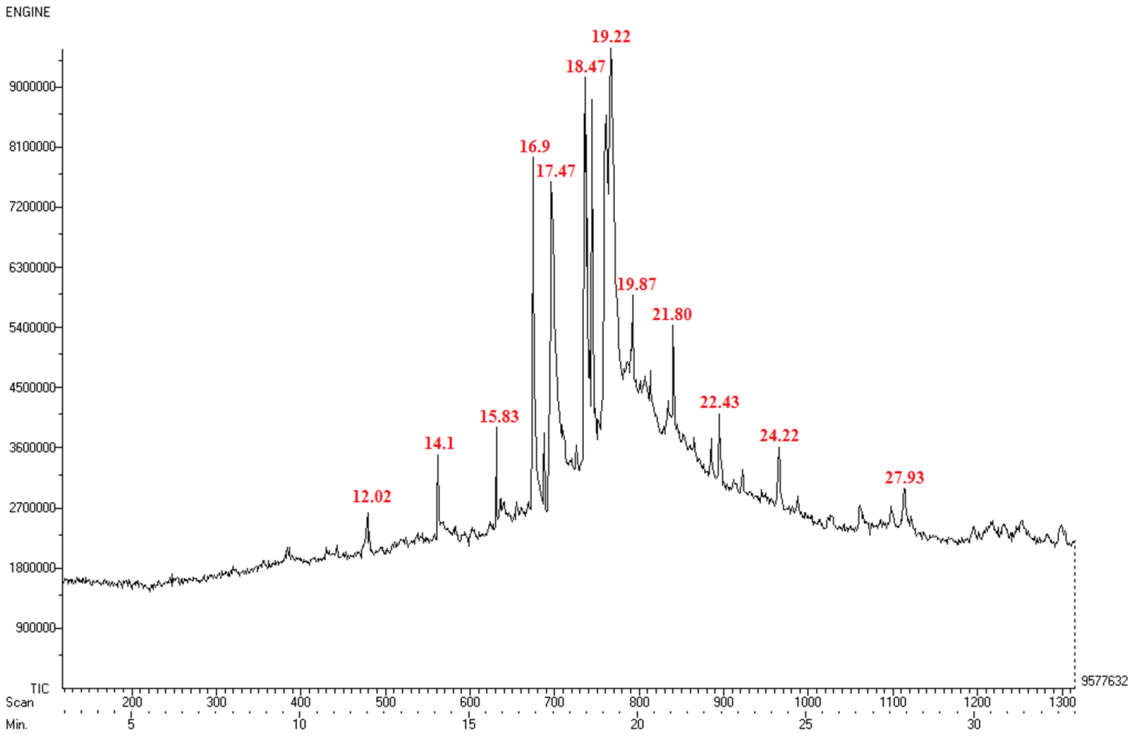


Figure 4. GC-MS for Citronella oil.

2.4. Characterization of $CoCr_2O_4$

2.4.1. XRD Analysis

An X-ray diffraction (XRD) test was conducted for phase identification of the prepared nano-cobalt chromite. The test results in a picture output to conform and verify the crystal structure of the material. Thus, for the prepared nano-cobalt chromite compound the XRD pattern was recorded by X-ray diffractometer, with copper employed as the target material (with Cu Kα as a diffraction source) to explore the sample. It can be seen that the output of the prepared cobalt chromite compound matches the simulated output well. However, an impurity phase screening at near ~33o belongs to a Cr_2O_3 (@), which means that the single-step synthesis of the Solution Combustion technique does not offer a greater pure phase of $CoCr_2O_4$ when major amounts of Cr ion are quickly oxidized to form Cr_2O_3 precipitate. The crystallite size of the prepared cobalt chromite was found to be ~22 nm as calculated by the Scherrer formula

$$Dp = \frac{0.94\lambda}{\beta 1/2\ cos\theta} \quad (1)$$

where D_p is the size of crystallite in nm, θ is the degree theta, and β is the radian.

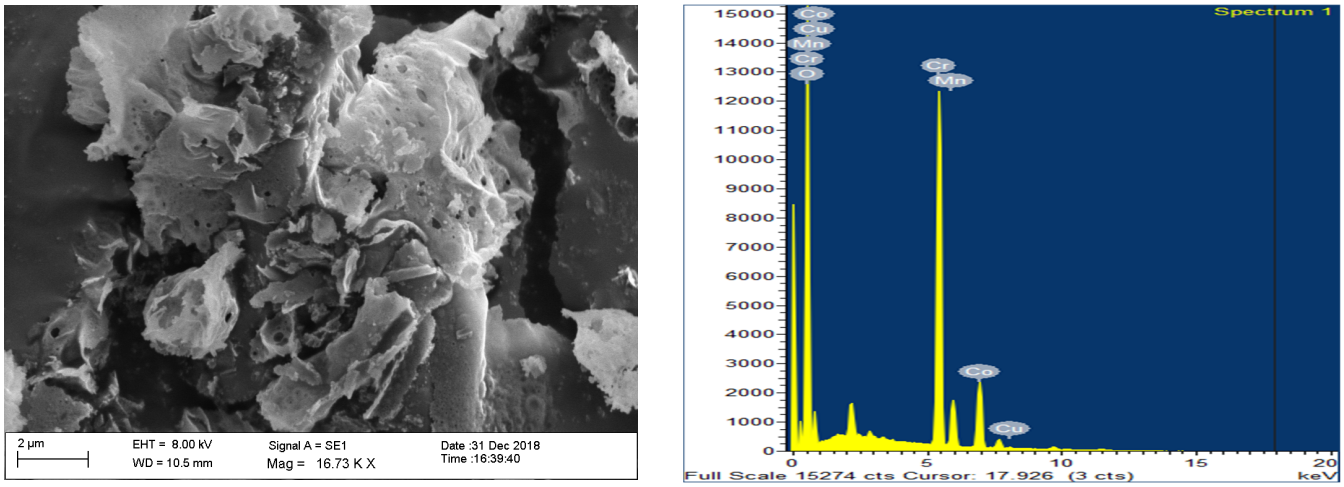
2.4.2. SEM Analysis

SEM microscopy was used for elemental analysis of the prepared cobalt chromite compound. Figure 5a is a pictorial representation of the SEM image of the prepared cobalt chromite compound from an SEM analyzer obtained using an X-ray spectrometer at magnification 20,000× to 167,000×. The experimental analysis was carried out at 8.00 kV and the acquired outcomes were a notable collection of particles with an important poriferous nature.

2.4.3. EDX Analysis

From the point of view of energy content, the content mass is quite natural, which allows the growth of crystallites. Figure 5b exemplifies the Energy Dispersive X-ray (EDX) spectrum of prepared the cobalt chromite compound, which shows that the cobalt, chromium, and

oxygen elements are present in the prepared cobalt chromite compound. It is manifest from the collected results that no impurities are present in the prepared $CoCr_2O_4$ composition. Figures 5 and 6 displays the recorded and simulated patterns of $COCr_2O_4$.



(**a**) (**b**)

Figure 5. (**a**) SEM Image and (**b**) EDX Spectra of nano-cobalt chromite.

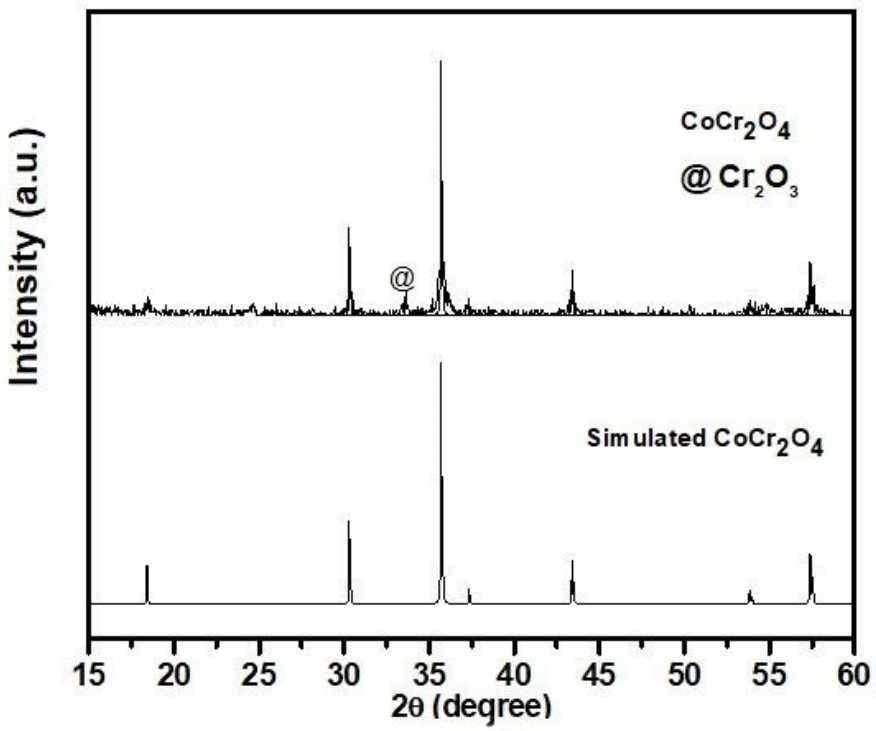


Figure 6. XRD for nano-cobalt chromite.

2.5. Test Fuel Preparation

In the current work, test fuel was prepared using two techniques. In the first technique, a nanoemulsion, fuel was prepared using water, an emulsifier, and nanopowder. In the second technique, the novel concept of RTEFI was introduced to prepare and supply the test fuel. The thermal property of test fuel is shown in Table 2.

Table 2. Thermal, physical, and chemical properties of test fuel.

Properties	D100 (100% Diesel)	B100 (100% Citronella)	SDE (Surfactant-Free Diesel Emulsion)	SBE (Surfactant-Free Bioemulsion)	SNBE (Surfactant-Free Nano-Bioemulsion)
Calorific Value (MJ/kg)	44.12	38	43.009	41.089	41.183
Cetane number	47	55	46	50	51
Kinematic Viscosity (cSt)	2.9	4.9	3.45	3.91	4.15
Flash Pt (°C)	66	55	68	64	66
Density (kg/m^3)	820	900	843	871	844

3. Configuration of the Test Ring

For further investigation, a one-cylinder conventional Kirloskar-made naturally aspirated steady speed direct injection diesel engine with a power output of 5.2 kW was used. The fuel tank was 6.5 L, with the air drawn inside the cylinder through the inlet manifold during the suction stroke. The detailed specifications of the engine are provided in Table 3.

Table 3. Engine specifications.

Make	Kirloskar TV-1
Type	Four-stroke engine
Cooling	Water
Bae Engine Bore	86.6 mm
Bae Engine Stroke	112 mm
Compression ratio	17.6:1
Power Rating	5.1 kW
Speed	1500 rpm
IT	23deg before TDC
Nozzle	0.3 mm and three nozzles
Bowl	Hemispherical

An inline mixing system, the RTEFI system, was attached close to the mechanical fuel injection structure. Pressure sensors were placed on the cylinder head to measure the combustion parameters.

A smoke analyzer and AVL DI gas analyzer were employed to quantify the tailpipe emissions. The emission analyzer specifications are sown in Table 4; Table 5 shows the Test Matrix.

Table 4. Emission analyzer specifications.

Instruments	Type	Manufacturer	Measuring Range	Standard Error
Smoke Meter	AVL Smoke meter	AVL India Pvt. Ltd. (Gurugram, India)	0 to 100 HSU	±0.1
Five-gas analyzer	Krypton 290 five-gas analyzer	SMS Auto Line Equipment Pvt. Ltd. (Chennai, India)	CO—(0–10%) CO_2—(0 to 20%) HC—(0 to10,000 ppm) O_2—(0 to 25%) NO_x—(0 to 5000 ppm)	±0.1 ±0.1 ±0.05 ±0.02

Table 5. Test matrix.

Test No.	Test Abbreviations	Load	Base Fuel	Water Concentration	Nanoadditive Concentration
1	D100	Variable 0–100% (Constant speed 1500 rpm, IT 23 degCA, IP 200 bar)	Diesel fuel (100%)	-	-
2	B100	Variable 0–100% (Constant speed 1500 rpm, IT 23 degCA, IP 200 bar)	Citronella fuel (100%)	-	-
3	SDE	Variable 0–100% (Constant speed 1500 rpm, IT 23 degCA, IP 200 bar)	Diesel (95%)	5%	-
4	SBE	Variable 0–100% (Constant speed 1500 rpm, IT 23 degCA, IP 200 bar)	Citronella fuel (25%) + Diesel (70%)	5%	-
5	SNBE	Variable 0–100% (Constant speed 1500 rpm, IT 23 degCA, IP 200 bar)	Citronella fuel (25%) + Diesel (70%)	5%	100 ppm

Ambiguity Examination

Commonly, error arises in an instrument due to factors such as instrument condition, environmental conditions, the type of observations being made, and the test procedure. Dissimilarity among instrument makers, calibration techniques, and data collection procedures can lead to experimental uncertainty. Uncertainty analysis is used to avoid variations in the experimental results. The ambiguity among diverse measuring instruments and parameters is shown in Table 6.

Table 6. Ambiguity examination.

S.no	Measured Parameters	Percent Uncertainty
1.	BTE	0.4%
2.	BSFC	0.6%
3.	Pressure	0.2%
4.	BP	0.4%
5.	Crank angle encoder	0.05%
6.	Engine Speed	0.1%
7.	Dynamometer Load	0.2%

4. Result and Discussion

4.1. Performance Output Response

Figure 7 shows the BTE for Diesel (D), Biofuel (B), surfactant-free diesel emulsion (SDE), surfactant-free bioemulsion (SBE), and surfactant-free nano-bioemulsion (SNBE) under diverse load states. From the graph, it can be seen that all the test fuels display increased BTE with increased engine loads. Both the SDE and SBE emulsions and the B fuel have lower BTE correlated with D. Nevertheless, SNBE fuel exhibits slightly higher BTE than SBE, which is due to the positive impact of the cobalt chromite additive [43,44]. There is significant improvement of BTE at high load conditions when fuelled with D, SDE, SBE, and SNBE, 2.22%, 1.26%, 1.64%, and 2.04%, respectively, compared to B100. Additionally, both emulsion fuels are combustible effectively because of micro-explosions and the secondary atomization of fuel. The BTE for D, SDE, SBNE, SBE, and B100 is 31.14%, 30.18%, 30.96%, 30.56%, and 28.92%, respectively, at peak load condition. This outcome might be a reason for the fast evaporation interaction of H_2O, which is at first introduced in oil drops as exceptionally fine beads, which positively influences the air/fuel fixing and thus enhances brake thermal efficiency. Another important result is that the emulsion fuels had a higher ignition lag, which allows sufficient duration to physically prepare the

test fuel. In addition, this result may be a positive influence on catalytic cracking of the hydrocarbon chain and the O_2 buffer property of cobalt chromite nanoparticles.

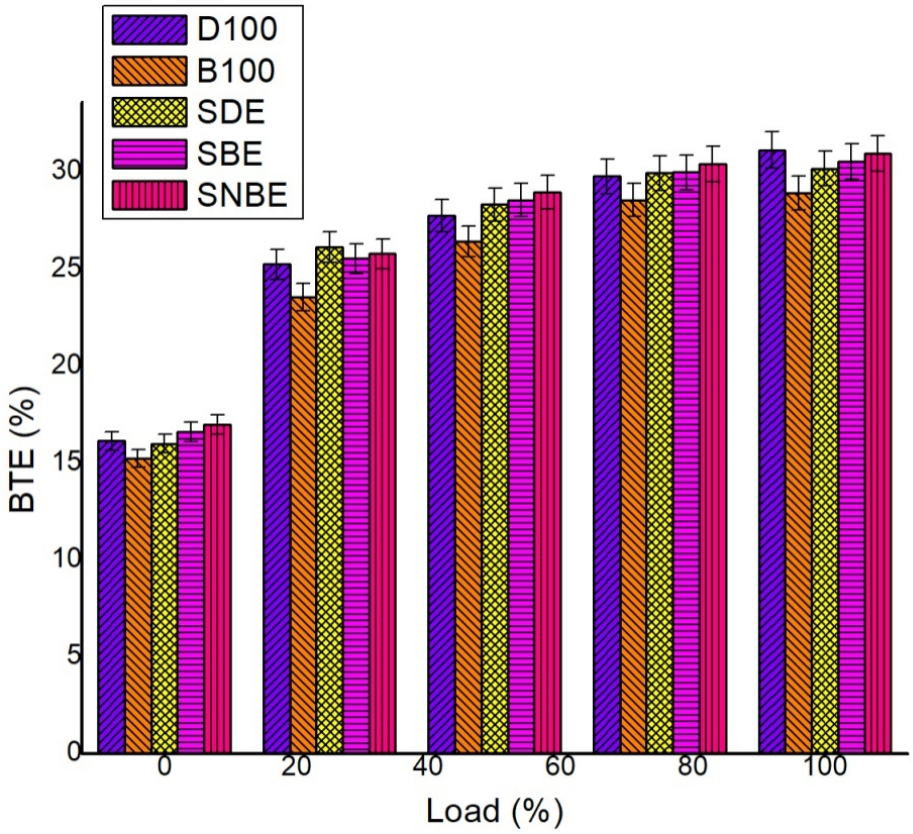


Figure 7. BTE vs. BP.

The BSFC is a significant parameter; it is an indicator that measures engine effectiveness and the amount of fuel utilization inside the engine to develop a certain power output. Figure 8 shows that the BSFC output for D, SDE, SBNE, SBE, and B100 is 292 kJ/kW-h, 326 kJ/kW-h, 302 kJ/kW-h, 312 kJ/kW-h, and 345 kJ/kW-h, respectively, at top load state. The D fuel had better fuel consumption than other test fuels due to the high heat content present in D fuel. There is a significant improvement in BSFC when fuelled with D, SDE, SBE, and SNBE, respectively, 15.36%, 5.51%, 9.57%, and 12.46% compared to B100 under high load conditions. These explanations are consistent with Krishnamoorthy et al. [9], where BFO and BFO emulsion fuel had poor BSFC when correlated with diesel. On the whole, the SNBE fuel exhibits considerable improvement in performance output response as a result of greater dispersion of cobalt chromite nanopowder at the combustion phase.

4.2. Emission Output Response

The nitrogen oxide emission evaluation of the adopted test fuel and contrast with diesel under diverse load states are shown in Figure 9. Generally, a CI engine emits more NO_x emission than the SI engine owing to the higher combustion temperature caused by the high oxygen presence inside the CC. The NO_x output for D, SDE, SBNE, SB, E and B is 849 ppm, 847 ppm, 824 ppm, 839 ppm, and 852 ppm, respectively, at the top load state. From the graph it can be seen that the B fuel delivers more NO_x emissions due to an enriched O_2 proportion. It can be seen that B fuel exhibits 50% greater nitrogen oxide formation relative to diesel at peak load state. At 10%, the water concentration in SBE lowers NO_x formation by 25% compared to pure B fuel at full load owing to LHV and higher ID of SBE. Furthermore, the addition of the nanoadditive in SBE promotes lower NO_x formation by about 10%. The SBNE blend exhibits the maximum NO_x reduction due to its positive property of a high surface area to volume ratio [45–48].

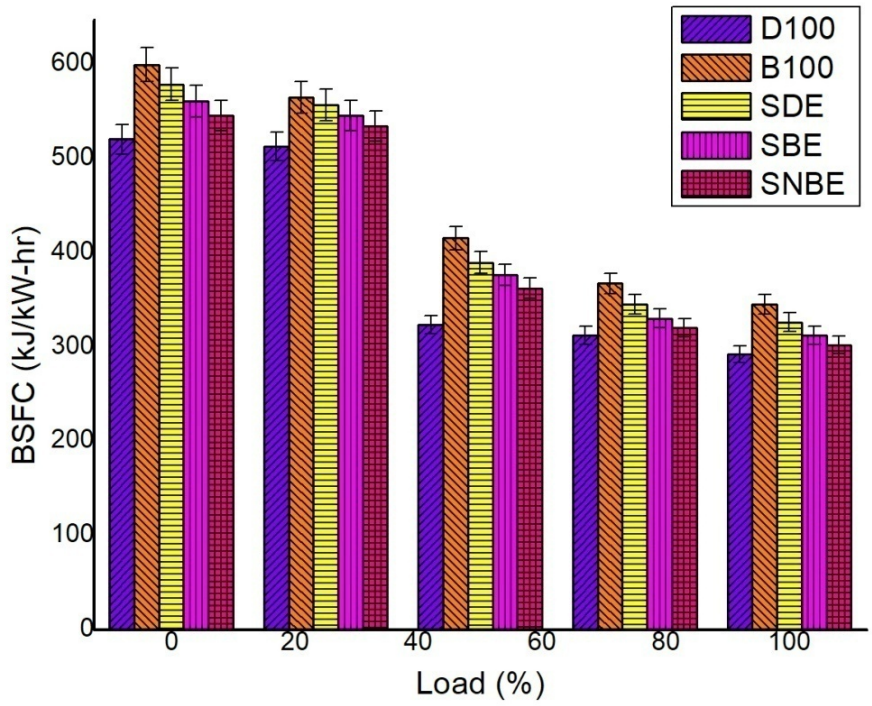


Figure 8. BSFC vs. BP.

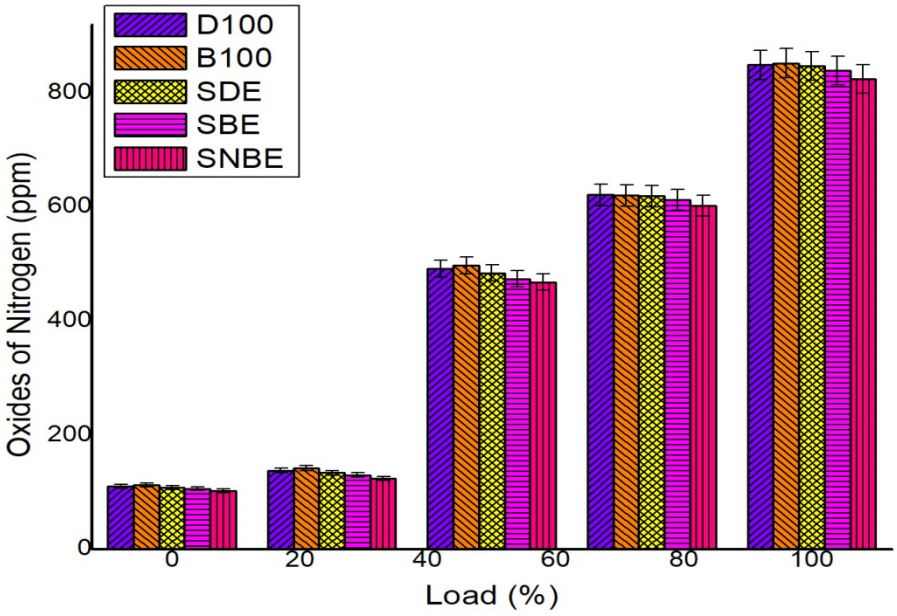


Figure 9. Nitrogen oxide emissions vs. brake power.

Figure 10 represents HC formation for Diesel (D), Biofuel (B), surfactant-free diesel emulsion (SDE), surfactant-free bioemulsion (SBE), and surfactant-free nano-bioemulsion (SNBE) under varied load states. The HC output for D, SDE, SBNE, SBE, and B is 76 ppm, 67 ppm, 58 ppm, 61 ppm, and 72 ppm, respectively, at the top load state. At low load, it can be seen that the B blend exhibits lower HC formation compared with other test fuels, as the B blend has higher O_2 and lower carbon content, which can enhance the proper process of combustion. On the other hand, the SBE blend had greater HC formation than the B blend due to the LHV of water present in the SBE blend, resulting in incomplete combustion. At high load states the SBE blend emits lower HC emission from the CI engine tailpipe than the B blend, owing to the positive impact of micro-explosions and secondary atomization [49–52]. The cobalt chromite nanoadditive added to the SBE blend

considerably reduce HC formation and positively enhance the ignition lag, heat transfer rate, and explosion rate, resulting in fully complete combustion. On the whole, at the maximum load condition the SBNE blend exhibits greater HC emission reduction than all other test fuels due to its positive property of a high surface area to volume ratio.

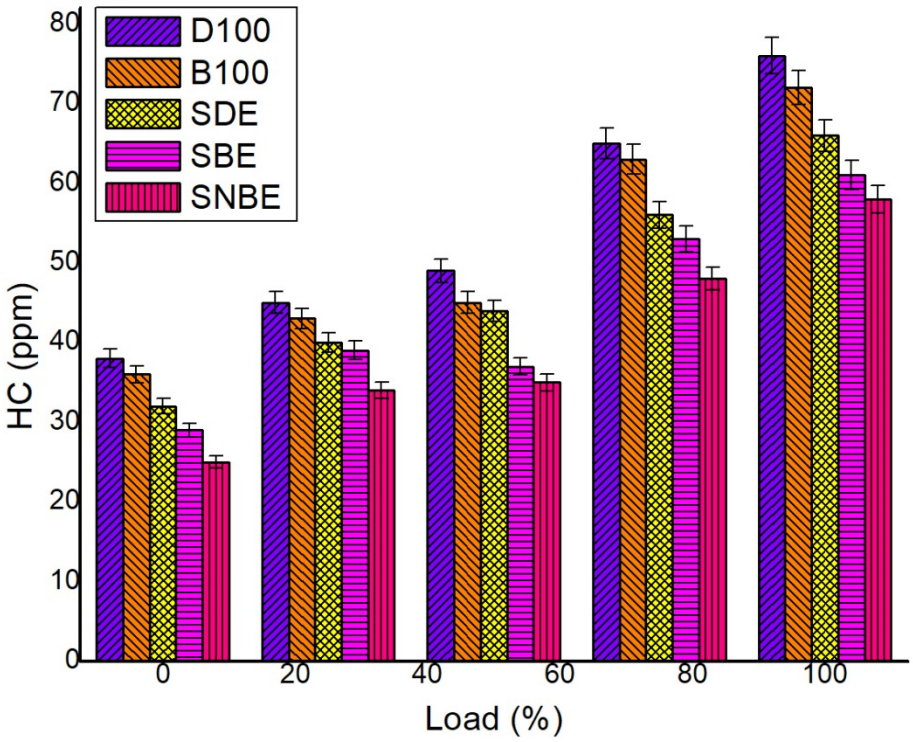


Figure 10. Hydrocarbon emissions vs. brake power.

Generally, the magnitude of CO formation was minimal in the CI engine compared with the SI engine. Usually, the formation of CO emissions depends on the air/fuel ratio in the IC engine. Figure 11 shows CO formation for Diesel (D), Biofuel (B), surfactant-free diesel emulsion (SDE), surfactant-free bioemulsion (SBE) and surfactant-free nano-bioemulsion (SNBE) at varied load ranges. CO decreased with increased engine loads from 0% to 100% for all the test fuels, owing to peak in-cylinder temperature being associated with higher load conditions. At high load state, the SBE blend emits lower CO emission from the CI engine tailpipe than the B blend, owing to the positive impact of micro-explosions and secondary atomization. The cobalt chromite nanoadditive added to the SBE blend considerably reduce CO formation and positively enhance the ignition lag, heat transfer rate, and explosion rate, ad resulting in fully complete combustion [53–56]. On the whole, at the maximum load condition the SBNE blend exhibits greater CO emissions reduction than all other test fuels due to its positive property of a high surface area to volume ratio.

Figure 12 shows the smoke formation for Diesel (D), Biofuel (B), surfactant-free diesel emulsion (SDE), surfactant-free bioemulsion (SBE), and surfactant-free nano-bioemulsion (SNBE) under varied load range. In order to uphold the constant speed of the engine under the all load states the engine allows the incremental fuel to burn, which influences smoke formation. The graph shows that the biofuels had lower smoke formation than diesel at all load states, which is due to the availability of the oxygen proportion in B fuel. Furthermore, the additional of water content in biofuel diminishes the smoke output compared to diesel thanks to improved atomization [57,58]. At a high load state, the SBE blend emits less smoke from the CI engine tailpipe than the B blend, owing to the positive impact of micro-explosions and secondary atomization. The cobalt chromite nanoadditive added to the SBE blend considerably reduces smoke formation and positively enhances the ignition lag, heat

transfer rate, and explosion rate, resulting in fully complete combustion [59–61]. On the whole, at the maximum load condition the SBNE blend exhibits greater smoke emission reduction than all other test fuels thanks to its positive property of a high surface area to volume ratio [62–64].

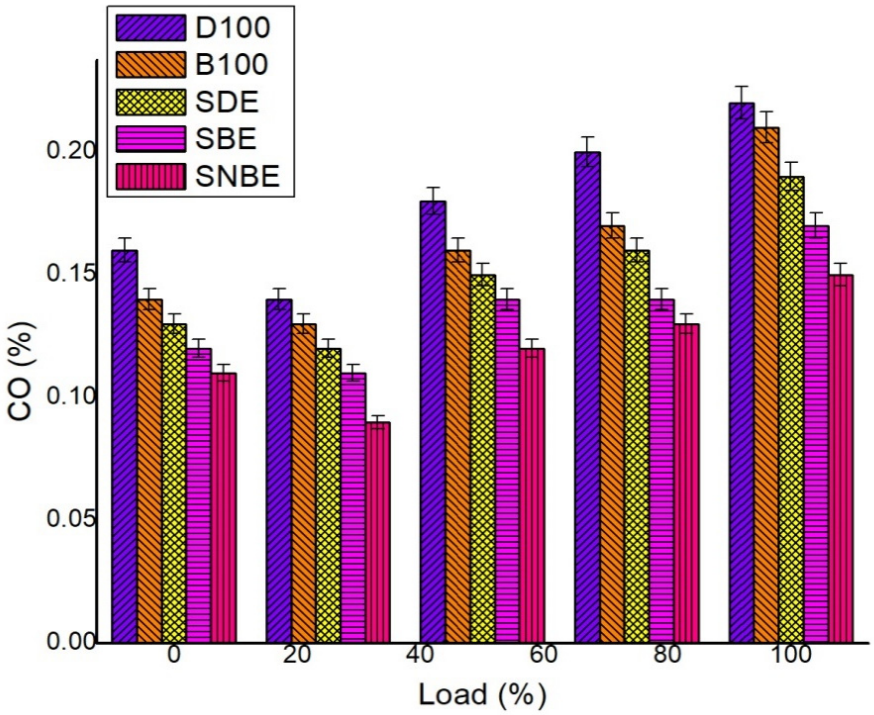


Figure 11. Carbon monoxide emissions vs. brake power.

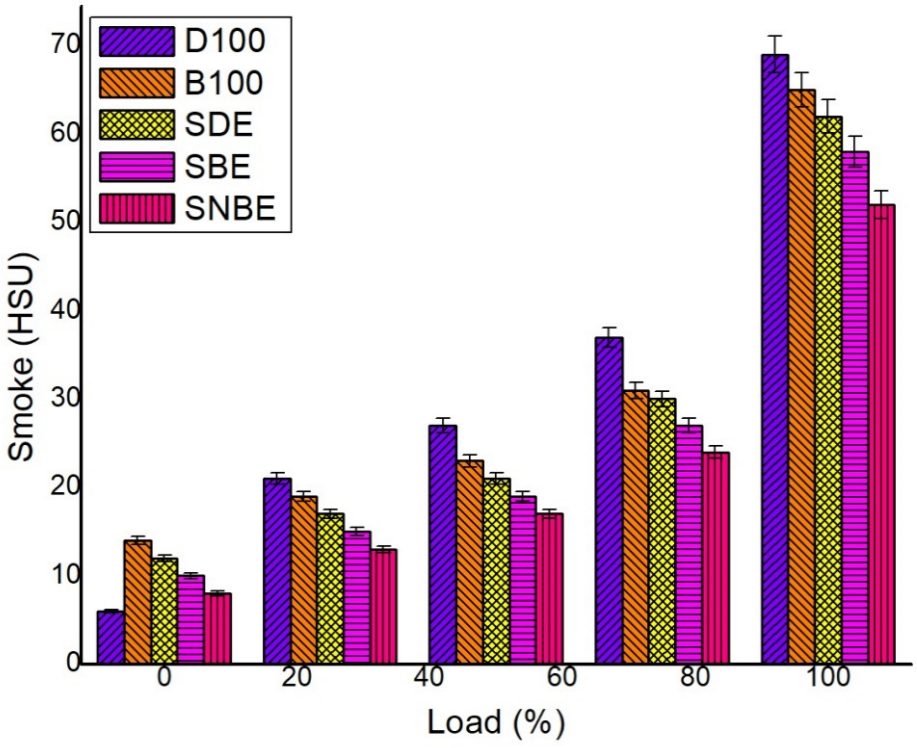


Figure 12. Smoke emissions vs. brake power.

4.3. Combustion Output Response

In a diesel engine the cylinder pressure commonly depends on various factors, namely, the equivalence rate, A/F rate, evaporation rate, ignition delay and CD period, and fuel burned separately during the premixed burning stage. Figure 13 shows the variation in Cylinder Pressure (CP) with respect to the crank angle for Diesel (D), Biofuel (B), surfactant-free diesel emulsion (SDE), surfactant-free bioemulsion (SBE), and surfactant-free nano-bioemulsion (SNBE) under varied load ranges. The maximum CP output for D, SDE, SBNE, SBE, and B100 is 65 bar, 67 bar, 61 bar, 64 bar, and 63 bar, respectively, at the top load state. Both SDE and SBE emulsion and B fuel show lower CP correlated to D due to the CV of D fuel. Nevertheless, SNBE fuel exhibits slightly higher CP than SBE due to the positive impact of cobalt chromite additive. Additionally, emulsion fuel combusts effectively thanks to secondary atomization and micro-explosions. This result may be a reason for the fast process of H_2O evaporation that is organically introduced in oil drop attacks as exceptionally fine drops, which influences air/fuel fixing and enhances brake thermal efficiency. Another important element of this result is that emulsion fuel has a higher ignition lag, which allows time to physically prepare the test fuel. This result may show a positive influence on catalytic cracking of the hydrocarbon chain and the O_2 buffer property of cobalt chromite nanoparticles [62–64].

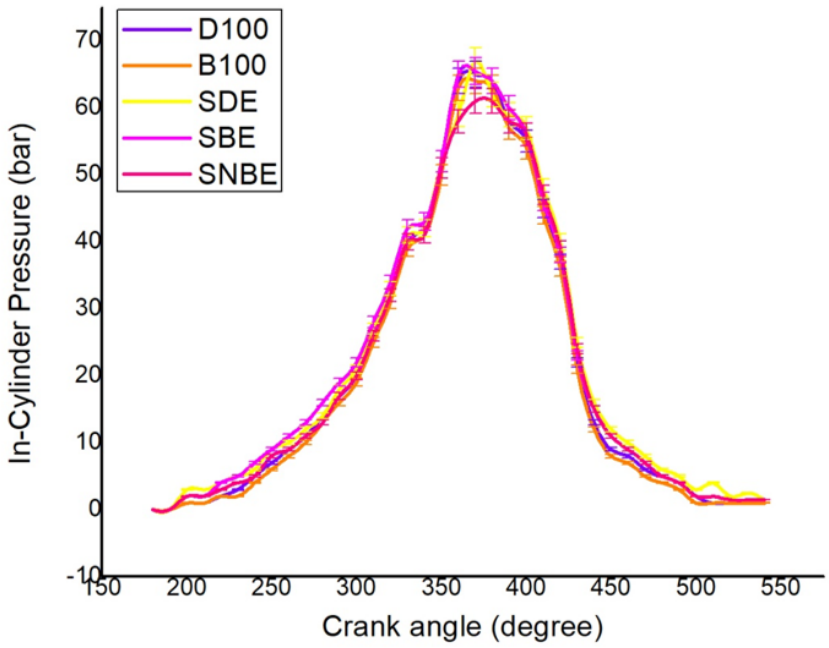


Figure 13. In-cylinder pressure vs. brake power.

HRR is the measure of heat radiated by most of the burn throughout the combustion stage inside the base engine cylinder. In the present work, the HRR was calculated from the CP with respect to the Crank angle (CA) using following the expression equation

$$\frac{dQnet}{d\theta} = \left(\frac{\gamma}{\gamma - 1} P \frac{dV}{d\theta}\right) + \left(\frac{1}{\gamma - 1} V \frac{dP}{d\theta}\right)$$

where:

$\frac{dQnet}{d\theta}$ = Net heat release rate in (kJ/m^3 CA);
V = Instantaneous volume in (m^3);
P = Instantaneous pressure in (bar);
γ = ratio of specific heat.

Figure 14 shows the variation in HRR with respect to the crank angle for Diesel (D), Biofuel (B), surfactant-free diesel emulsion (SDE), surfactant-free bioemulsion (SBE), and surfactant-free nano-bioemulsion (SNBE) under varied load ranges. Both SDE and SBE emulsion and B fuel show lower CP correlated to D due to the CV of D fuel. Nevertheless, SNBE fuel exhibits a slightly higher HRR than SBE due to the positive impact of the cobalt chromite additive.

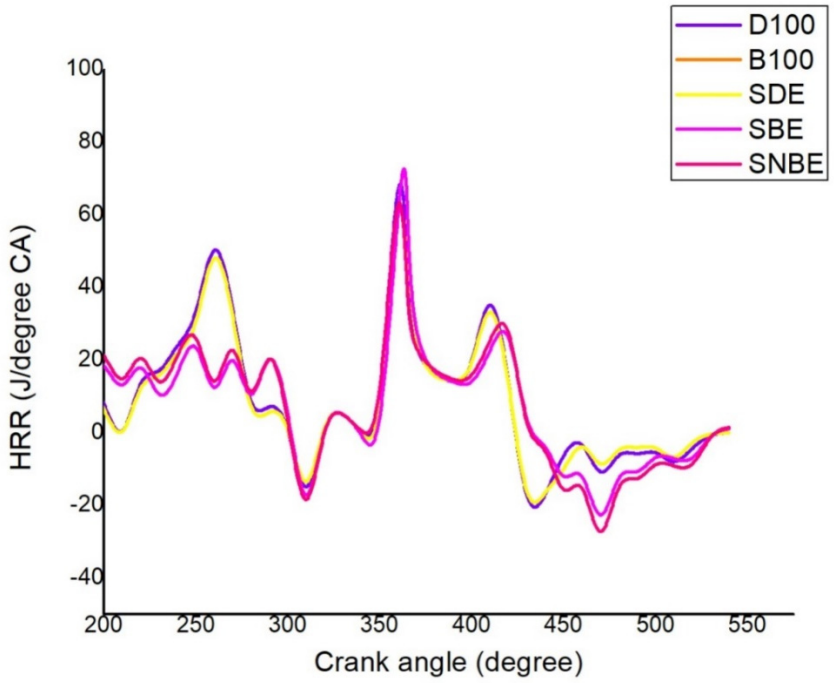


Figure 14. Heat release rate vs. brake power.

5. Conclusions

The performance, emissions, and combustion of citronella biodiesel blended with water and a nanoadditive were investigated in a single-cylinder diesel engine with attached RTEFI. The obtained conclusions are listed below.

- The BTE of the engine was enhanced with SBE fuel by 1.64% and with SNBE fuel by 2.04% compared to unadulterated Citronella fuel at the most extreme load range. In all cases, conventional fuel activity displayed the greatest BTE compared to all other test fuels
- At the maximum load range, the BSFC of the engine was enhanced with SBE and SNBE fuel by 9.57% and 12.46%, respectively, compared to pure Citronella fuel. and was. The respective BSFC for the D, SDE, SBE, and SNBE fuels was 292 kJ/kW-h, 326 kJ/kW-h, 312 kJ/kW-h, and 302 kJ/kW-h.
- The SDE, B100, SBE, and SNBE fuels had a significantly reduced HC in the tailpipe, by 13.16%, 5.27%, 19.75%, and 23.68%, respectively, and CO in the tailpipe. by 13.65%), (4.54%), (22.73%), and (31.82%), respectively, compared with conventional diesel fuel at the peak load condition. However, the SDE blend exhibited higher HC and CO emissions than Diesel fuel.
- At all load ranges, the NO_x emission trend was lower for SBE than for diesel and the SDE blend (by 1.18% and 2.95%, respectively) as well as for SNBE (by 0.94% and 2.72%, respectively). However, pure citronella fuel showed greater NO_x formation than SBE fuel.
- A significant improvement in the opacity of smoke was noted for both emulsion bio-fuels relative to B100 fuel, with a respective decrease of 10.77% and 20%, while

Diesel fuel had increased smoke formation compared to both the nanoemulsion and emulsion fuels.

- CP and HRR increased for both nanoemulsion and emulsion SBE and SBNE fuels compared to convention diesel fuel; however, B100 fuel had minimal CP and HRR compared to Diesel fuel.

Author Contributions: Conceptualization, K.R., A.A. and M.B.; Data curation, E.P.V.; Investigation, K.R.; Methodology, K.R. and E.P.V.; Software, E.P.V.; Supervision, E.P.V. and M.B.; Validation, A.A.; Visualization, A.A.; Writing—original draft, K.R.; Writing—review & editing, A.A. and M.B. All authors have read and agreed to the published version of the manuscript.

Funding: This research is supported by the Structures and Materials (S&M) Research Lab of Prince Sultan University and the authors acknowledge the support of Prince Sultan University for paying the article processing charges (APC) of this publication.

Institutional Review Board Statement: Not applicable.

Informed Consent Statement: Not applicable.

Data Availability Statement: Not applicable.

Acknowledgments: The authors would like to express heartful thanks to S. Saravanan, Principal, CK College of Engineering and Technology, Cuddalore. The authors thank K. Annamalai, Automobile Department, MIT, Anna University, Chromepet and Chennai 44 for allowing us to utilize the Engine Research Lab for this work.

Conflicts of Interest: The authors declare no conflict of interest.

Abbreviations

CI	Compression Ignition
DI	Direct Injection
CO	Carbon monoxide
NO_x	Nitrogen oxides
CO_2	Carbon dioxide
HC	Hydrocarbon
BSEC	Brake Specific Energy Consumption
BTE	Brake Thermal Efficiency
ID	Ignition Delay
CN	Cetane Number
ASTM	American Society for Testing and Materials
BP	Brake power
TFC	Total fuel consumption
HRR	Heat Release Rate
UBHC	Unburned Hydrocarbon
H_2O	Water
HSU	Hartridge Smoke Units
O_2	Oxygen
CA	Crank Angle
LGO	Lemongrass Oil
WCO	Waste Cooking Oil
GC-MS	Gas Chromatography-Mass Spectrometry
FT-IR	Fourier Transform Infrared spectroscopy
USIA	United State Energy Information Administration
RTEFI	Real Time Emulsion Fuel Injection

References

1. Zou, C.; Zhao, Q.; Zhang, G.; Xiong, B. Energy revolution: From a fossil energy era to a new energy era. *Nat. Gas Ind. B* **2016**, *3*, 1–11. [CrossRef]
2. Ramalingam, K.; Balasubramanian, D.; Chellakumar, P.J.T.J.S.; Padmanaban, J.; Murugesan, P.; Xuan, T. An assessment on production and engine characterization of a novel environment-friendly fuel. *Fuel* **2020**, *279*, 118558. [CrossRef]
3. Venu, H.; Madhavan, V. Influence of diethyl ether (DEE) addition in ethanol-biodiesel-diesel (EBD) and methanol-biodiesel-diesel (MBD) blends in a diesel engine. *Fuel* **2017**, *189*, 377–390. [CrossRef]
4. Agarwal, A.K. Biofuels (alcohols and biodiesel) applications as fuels for internal combustion engines. *Prog. Energy Combust. Sci.* **2007**, *33*, 233–271. [CrossRef]
5. Bezergianni, S.; Dimitriadis, A. Comparison between different types of renewable diesel. *Renew. Sustain. Energy Rev.* **2013**, *21*, 110–116. [CrossRef]
6. Ashok, B.; Nanthagopal, K.; Chaturvedi, B.; Sharma, S.; Raj, R.T.K. A comparative assessment on Common Rail Direct Injection (CRDI) engine characteristics using low viscous biofuel blends. *Appl. Therm. Eng.* **2018**, *145*, 494–506. [CrossRef]
7. Ramalingam, K.; Kandasamy, A.; Balasubramanian, D.; Palani, M.; Subramanian, T.; Varuvel, E.G.; Viswanathan, K. Forcasting of an ANN model for predicting behaviour of diesel engine energised by a combination of two low viscous biofuels. *Environ. Sci. Pollut. Res.* **2019**, *27*, 24702–24722. [CrossRef] [PubMed]
8. Kumar, J.R.; Vikram, C.J.; Naveenchandran, P. Investigation for the performance and emission test using citronella oil in single cylinder diesel engine. *Middle East J. Sci. Res.* **2012**, *12*, 1754–1757.
9. Hoekman, S.K.; Broch, A.; Robbins, C.; Ceniceros, E.; Natarajan, M. Review of biodiesel composition, properties, and specifications. *Renew. Sustain. Energy Rev.* **2012**, *16*, 143–169. [CrossRef]
10. Atabani, A.; Silitonga, A.; Badruddin, I.A.; Mahlia, T.M.I.; Masjuki, H.; Mekhilef, S. A comprehensive review on biodiesel as an alternative energy resource and its characteristics. *Renew. Sustain. Energy Rev.* **2012**, *16*, 2070–2093. [CrossRef]
11. Ramalingam, K.; Kandasamy, A.; Subramani, L.; Balasubramanian, D.; Thadhani, J.P.J. An assessment of combustion, performance characteristics and emission control strategy by adding anti-oxidant additive in emulsified fuel. *Atmos. Pollut. Res.* **2018**, *9*, 959–967. [CrossRef]
12. Hoekman, S.K.; Robbins, C. Review of the effects of biodiesel on NO_x emissions. *Fuel Process. Technol.* **2012**, *96*, 237–249. [CrossRef]
13. Al-Dawody, M.; Bhatti, S. Optimization strategies to reduce the biodiesel NO_x effect in diesel engine with experimental verification. *Energy Convers. Manag.* **2013**, *68*, 96–104. [CrossRef]
14. Ramalingam, K.; Kandasamy, A.; Chellakumar, P.J.T.J.S. Production of eco-friendly fuel with the help of steam distillation from new plant source and the investigation of its influence of fuel injection strategy in diesel engine. *Environ. Sci. Pollut. Res.* **2019**, *26*, 15467–15480. [CrossRef] [PubMed]
15. Elsanusi, O.A.; Roy, M.M.; Sidhu, M.S. Experimental Investigation on a Diesel Engine Fueled by Diesel-Biodiesel Blends and their Emulsions at Various Engine Operating Conditions. *Appl. Energy* **2017**, *203*, 582–593. [CrossRef]
16. Vigneswaran, R.; Annamalai, K.; Dhinesh, B.; Krishnamoorthy, R. Experimental investigation of unmodified diesel engine performance, combustion and emission with multipurpose additive along with water-in-diesel emulsion fuel. *Energy Convers. Manag.* **2018**, *172*, 370–380. [CrossRef]
17. Leng, L.; Chen, J.; Leng, S.; Li, W.; Huang, H.; Li, H.; Yuan, X.; Li, J.; Zhou, W. Surfactant assisted upgrading fuel properties of waste cooking oil biodiesel. *J. Clean. Prod.* **2019**, *210*, 1376–1384. [CrossRef]
18. Lin, C.-Y.; Lin, S.A. Effects of emulsification variables on fuel properties of two-and three-phase biodiesel emulsions. *Fuel* **2007**, *86*, 210–217. [CrossRef]
19. Vellaiyan, S.; Amirthagadeswaran, K.S. Zinc oxide incorporated water-in-diesel emulsion fuel: Formulation, particle size measurement, and emission characteristics assessment. *Pet. Sci. Technol.* **2016**, *34*, 114–122. [CrossRef]
20. Musculus, M.P.B.; Dec, J.E.; Tree, D.R.; Daly, D.; Langer, D.; Ryan, T.W., III; Matheaus, A.C. Effects of water-fuel emulsions on spray and combustion processes in a heavy-duty DI diesel engine. *SAE Trans.* **2002**, *111*, 2736–2756. [CrossRef]
21. Ithnin, A.M.; Yahya, W.; Ahmad, M.A.; AtiqahRamlan, N.; Kadir, H.A.; Sidik, N.A.C.; Koga, T. Emulsifier-free Water-in-Diesel emulsion fuel: Its stability behaviour, engine performance and exhaust emission. *Fuel* **2018**, *215*, 454–462. [CrossRef]
22. Vellaiyan, S. Enhancement in combustion, performance, and emission characteristics of a biodiesel-fueled diesel engine by using water emulsion and nanoadditive. *Renew. Energy* **2020**, *145*, 2108–2120. [CrossRef]
23. Vellaiyan, S.; Subbiah, A.; Chockalingam, P. Combustion, performance, and emission analysis of diesel engine fueled with water-biodiesel emulsion fuel and nanoadditive. *Environ. Sci. Pollut. Res.* **2018**, *25*, 33478–33489. [CrossRef] [PubMed]
24. Jeryrajkumar, L.; Anbarasu, G.; Elangovan, T. Effects on nanoadditives on performance and emission characteristics of calophyllum inophyllum biodiesel. *Int. J. Chem. Tech. Res.* **2016**, *9*, 210–219.
25. Soudagar, M.E.M.; Nik-Ghazali, N.-N.; Kalam, A.; Badruddin, I.A.; Banapurmath, N.R.; Akram, N. The effect of nano-additives in diesel-biodiesel fuel blends: A comprehensive review on stability, engine performance and emission characteristics. *Energy Convers. Manag.* **2018**, *178*, 146–177. [CrossRef]
26. Chandrasekaran, V.; Arthanarisamy, M.; Nachiappan, P.; Dhanakotti, S.; Moorthy, B. The role of nanoadditives for biodiesel and diesel blended transportation fuels. *Transp. Res. Part D Transp. Environ.* **2016**, *46*, 145–156. [CrossRef]

27. Saravankumar, P.T.; Suresh, V.; Vijayan, V.; Antony, G. Ecological effect of corn oil biofuel with SiO_2 nano-additives. *Energy Sources Part A: Recover. Util. Environ. Eff.* **2019**, *41*, 2845–2852. [CrossRef]
28. Krishnamoorthy, R.; Asaithambi, K.; Balasubramanian, D.; Murugesan, P.; Rajarajan, A. *Effect of Cobalt Chromite on the Investigation of Traditional CI Engine Powered with Raw Citronella Fuel for the Future Sustainable Renewable Source*; No. 2020-28-0445; SAE Technical Paper; SAE: Warrendale, PA, USA, 2020.
29. Gad, M.; Jayaraj, S. A comparative study on the effect of nano-additives on the performance and emissions of a diesel engine run on Jatropha biodiesel. *Fuel* **2020**, *267*, 117168. [CrossRef]
30. Hoseini, S.; Najafi, G.; Ghobadian, B.; Ebadi, M.; Mamat, R.; Yusaf, T. Performance and emission characteristics of a CI engine using graphene oxide (GO) nano-particles additives in biodiesel-diesel blends. *Renew. Energy* **2019**, *145*, 458–465. [CrossRef]
31. Kumar, S.; Dinesha, P.; Ajay, C.M.; Kabbur, P. Combined effect of oxygenated liquid and metal oxide nanoparticle fuel additives on the combustion characteristics of a biodiesel engine operated with higher blend percentages. *Energy* **2020**, *197*, 117194. [CrossRef]
32. Devarajan, Y.; Munuswamy, D.B.; Mahalingam, A. Investigation on behavior of diesel engine performance, emission, and combustion characteristics using nano-additive in neat biodiesel. Heat Mass Transf und Stoffuebertragung. *Heat Mass Transf.* **2019**, *55*, 1641–1650. [CrossRef]
33. Radhakrishnan, S.; Munuswamy, D.B.; Devarajan, Y.; Mahalingam, A. Performance, emission and combustion study on neat biodiesel and water blends fuelled research diesel engine. Heat Mass Transf und Stoffuebertragung. *Heat Mass Transf.* **2019**, *55*, 1229–1237. [CrossRef]
34. Dhinesh, B.; Annamalai, M. A study on performance, combustion and emission behaviour of diesel engine powered by novel nano nerium oleander biofuel. *J. Clean. Prod.* **2018**, *196*, 74–83. [CrossRef]
35. Yuvarajan, D.; Babu, M.D.; BeemKumar, N.; Kishore, P.A. Experimental investigation on the influence of titanium dioxide nanofluid on emission pattern of biodiesel in a diesel engine. *Atmos. Pollut. Res.* **2018**, *9*, 47–52. [CrossRef]
36. Venkata, R.M.; Yuvarajan, D. Emission analysis on the influence of magnetite nanofluid on methyl ester in diesel engine. *Atmos Pollut. Res.* **2016**, *7*, 477–481. [CrossRef]
37. Dhahad, H.A.; Chaichan, M.T. The impact of adding nano-Al2O3 and nano-ZnO to Iraqi diesel fuel in terms of compression ignition engines' performance and emitted pollutants. *Therm. Sci. Eng. Prog.* **2020**, *18*, 100535. [CrossRef]
38. Basha, J.S. Impact of Carbon Nanotubes and Di-Ethyl Ether as additives with biodiesel emulsion fuels in a diesel engine—An experimental investigation. *J. Energy Inst.* **2016**, *91*, 289–303. [CrossRef]
39. Sathiyamoorthi, R.; Sankaranarayanan, G. Effect of antioxidant additives on the performance and emission characteristics of a DICI engine using neat lemongrass oil–diesel blend. *Fuel* **2016**, *174*, 89–96. [CrossRef]
40. Bora, P.; Boro, J.; Konwar, L.J.; Deka, D. Formulation of microemulsion based hybrid biofuel from waste cooking oil—A comparative study with biodiesel. *J. Energy Inst.* **2016**, *89*, 560–568. [CrossRef]
41. Vinukumar, K.; Azhagurajan, A.; Vettivel, S.C.; Vedaraman, N. Rice husk as nanoadditive in diesel–biodiesel fuel blends used in diesel engine. *J. Therm. Anal.* **2018**, *131*, 1333–1343. [CrossRef]
42. Kareemullah, M.; Afzal, A.; Rehman, K.F.; Shahapurkar, K.; Khan, H.; Akram, N. Performance and emission analysis of compression ignition engine using biodiesels from Acid oil, Mahua oil, and Castor oil. *Heat Transf.* **2019**, *49*, 858–871. [CrossRef]
43. Afzal, A.; Mujeebu, M.A. Thermo-Mechanical and Structural Performances of Automobile Disc Brakes: A Review of Numerical and Experimental Studies. *Arch. Comput. Methods Eng.* **2019**, *26*, 1489–1513. [CrossRef]
44. Samuel, O.D.; Okwu, M.; Oyejide, O.J.; Taghinezhad, E.; Afzal, A.; Kaveh, M. Optimizing biodiesel production from abundant waste oils through empirical method and grey wolf optimizer. *Fuel* **2020**, *281*, 118701. [CrossRef]
45. Kumar, S.S.; Rajan, K.; Mohanavel, V.; Ravichandran, M.; Rajendran, P.; Rashedi, A.; Sharma, A.; Khan, S.A.; Afzal, A. Combustion, Performance, and Emission Behaviors of Biodiesel Fueled Diesel Engine with the Impact of Alumina Nanoparticle as an Additive. *Sustainability* **2021**, *13*, 12103. [CrossRef]
46. Aneeque, M.; Alshahrani, S.; Kareemullah, M.; Afzal, A.; Saleel, C.; Soudagar, M.; Hossain, N.; Subbiah, R.; Ahmed, M. The Combined Effect of Alcohols and *Calophylluminophyllum* Biodiesel Using Response Surface Methodology Optimization. *Sustainability* **2021**, *13*, 7345. [CrossRef]
47. Ağbulut, Ü.; Sarıdemir, S.; Rajak, U.; Polat, F.; Afzal, A.; Verma, T.N. Effects of high-dosage copper oxide nanoparticles addition in diesel fuel on engine characteristics. *Energy* **2021**, *229*, 120611. [CrossRef]
48. Razzaq, L.; Mujtaba, M.; Soudagar, M.E.M.; Ahmed, W.; Fayaz, H.; Bashir, S.; Fattah, I.R.; Ong, H.C.; Shahapurkar, K.; Afzal, A.; et al. Engine performance and emission characteristics of palm biodiesel blends with graphene oxide nanoplatelets and dimethyl carbonate additives. *J. Environ. Manag.* **2021**, *282*, 111917. [CrossRef]
49. Samuel, O.D.; Samuel, O.D.; Waheed, M.A.; Waheed, M.A.; Taheri-Garavand, A.; Taheri-Garavand, A.; Verma, T.N.; Verma, T.N.; Dairo, O.U.; Dairo, O.U.; et al. Prandtl number of optimum biodiesel from food industrial waste oil and diesel fuel blend for diesel engine. *Fuel* **2020**, *285*, 119049. [CrossRef]
50. Ağbulut, Ü.; Elibol, E.; Demirci, T.; Sarıdemir, S.; Gürel, A.E.; Rajak, U.; Afzal, A.; Verma, T.N. Synthesis of graphene oxide nanoparticles and the influences of their usage as fuel additives on CI engine behaviors. *Energy* **2021**, *244*, 122603. [CrossRef]
51. Yaliwal, V.; Banapurmath, N.; Soudagar, M.E.M.; Afzal, A.; Ahmadi, P. Effect of manifold and port injection of hydrogen and exhaust gas recirculation (EGR) in dairy scum biodiesel—low energy content gas-fueled CI engine operated on dual fuel mode. *Int. J. Hydrogen Energy* **2021**, *47*, 6873–6897. [CrossRef]

52. Khandal, S.V.; Ağbulut, Ü.; Afzal, A.; Sharifpur, M.; Razak, K.A.; Khalilpoor, N. Influences of hydrogen addition from different dual-fuel modes on engine behaviors. *Energy Sci. Eng.* **2022**, *10*, 881–891. [CrossRef]
53. Wategave, S.; Banapurmath, N.; Sawant, M.; Soudagar, M.E.M.; Mujtaba, M.; Afzal, A.; Basha, J.; Alazwari, M.A.; Safaei, M.R.; Elfasakhany, A.; et al. Clean combustion and emissions strategy using reactivity controlled compression ignition (RCCI) mode engine powered with CNG-Karanja biodiesel. *J. Taiwan Inst. Chem. Eng.* **2021**, *124*, 116–131. [CrossRef]
54. Arunkumar, M.; Mohanavel, V.; Afzal, A.; Sathish, T.; Ravichandran, M.; Khan, S.; Abdullah, N.; Bin Azami, M.; Asif, M. A Study on Performance and Emission Characteristics of Diesel Engine Using Ricinus Communis (Castor Oil) Ethyl Esters. *Energies* **2021**, *14*, 4320. [CrossRef]
55. Verma, T.N.; Rajak, U.; Dasore, A.; Afzal, A.; Manokar, A.M.; Aabid, A.; Baig, M. Experimental and empirical investigation of a CI engine fuelled with blends of diesel and roselle biodiesel. *Sci. Rep.* **2021**, *11*, 23. [CrossRef] [PubMed]
56. Elumalai, P.V.; Parthasarathy, M.; Hariharan, V.; Jayakar, J.; Iqbal, S.M. Evaluation of water emulsion in biodiesel for engine performance and emission characteristics. *J. Therm. Anal.* **2022**, *147*, 4285–4301. [CrossRef]
57. Sivakandhan, C.; Elumalai, P.V.; Murugan, M.; Saravanan, A.; Ranjit, P.S.; Varaprasad, B.; Murugan, M. Effects of on MnO_2 nanoparticles behavior of a sardine oil methyl ester operated in thermal barrier coated engine. *J. Therm. Anal.* **2022**, 13. [CrossRef]
58. Elumalai, P.V.; Senthur, N.S.; Parthasarathy, M.; Das, S.K.; Samuel, O.D.; Reddy, M.S.; Saravana, A.; Anjanidevi, S.; Sitaramamurty, A.S.; Anusha, M.; et al. Hydrogen in Spark Ignition Engines. In *Application of Clean Fuels in Combustion Engines. Energy, Environment, and Sustainability*; Di Blasio, G., Agarwal, A.K., Belgiorno, G., Shukla, P.C., Eds.; Springer: Singapore, 2022. [CrossRef]
59. Afzal, A.; Samee, A.D.M.; Javad, A.; Shafvan, S.A.P.V.A.; Kabeer, K.M.A. Heat transfer analysis of plain and dimpled tubes with different spacings. *Heat Transf. Asian Res.* **2017**, *47*, 556–568. [CrossRef]
60. Soudagar, M.E.M.; Kalam, M.A.; Sajid, M.U.; Afzal, A.; Banapurmath, N.R.; Akram, N.; Mane, S.; Saleel, A.C. Thermal analyses of minichannels and use of mathematical and numerical models. *Numer. Heat Transfer. Part A Appl.* **2020**, *77*, 497–537. [CrossRef]
61. Afzal, A.; Samee, A.D.M.; Razak, R.K.A.; Ramis, M.K. Steady and Transient State Analyses on Conjugate Laminar Forced Convection Heat Transfer. *Arch. Comput. Methods Eng.* **2020**, *27*, 135–170. [CrossRef]
62. Afzal, A.; Samee, A.M.; Jilte, R.; Islam, T.; Manokar, A.M.; Razak, K.A. Battery thermal management: An optimization study of parallelized conjugate numerical analysis using Cuckoo search and Artificial bee colony algorithm. *Int. J. Heat Mass Transf.* **2020**, *166*, 120798. [CrossRef]
63. Elumalai, P.V.; Dhinesh, B.; Jayakar, J.; Nambiraj, M.; Hariharan, V. Effects of antioxidants to reduce the harmful pollutants from diesel engine using preheated palm oil–diesel blend. *J. Therm. Anal. Calorim.* **2022**, *147*, 2439–2453. [CrossRef]
64. Elumalai, P.V.; Senthur, N.S.; Parthasarathy, M.; Dash, S.K.; Samuel, O.D.; Reddy, M.S.; Murugan, M.; Das, P.K.; Sitaramamurty, A.S.S.M.; Anjanidevi, S.; et al. Effectiveness of Hydrogen and Nanoparticles Addition in Eucalyptus Biofuel for Improving the Performance and Reduction of Emission in CI Engine. In *Greener and Scalable E-fuels for Decarbonization of Transport. Energy, Environment, and Sustainability*; Agarwal, A.K., Valera, H., Eds.; Springer: Singapore, 2022. [CrossRef]